Journal of Magnetic Resonance 317 (2020) 106778

Contents lists available at ScienceDirect

Journal of Magnetic Resonance

journal homepage: www.elsevier.com/locate/jmr

Monograph

A temperature-controlled sample shuttle for field-cycling NMR

Andrew M.R. Hall, Topaz A.A. Cartlidge, Giuseppe Pileio *

University of Southampton, Highfield Campus, Southampton SO17 1BJ, United Kingdom

ARTICLE INFO

Article history:
Received 6 May 2020
Revised 10 June 2020
Accepted 23 June 2020
Available online 27 June 2020

Keywords:
Field-cycling NMR
Sample shuttle
Singlet NMR
Spin relaxation

ABSTRACT

We present a design for a temperature-controlled sample shuttle for use in NMR measurements at variable magnetic field strength. Accurate temperature control was achieved using a mixture of water-ethylene glycol as a heat transfer fluid, reducing temperature gradients across the sample to < 0.05 °C and minimising convection. Using the sample shuttle, we show how the longitudinal (T_1) and singlet order (T_S) relaxation time constants were measured for two molecules capable of supporting long-lived states, with new record lifetimes observed at low field and above ambient temperatures.

1. Introduction

Many physical parameters important in NMR spectroscopy exhibit strong temperature and magnetic field dependencies which can be utilised to investigate underlying relaxation mechanisms and molecular dynamics. NMR relaxometry measurements at variable magnetic field strength (dispersion measurements) are frequently used to study molecular dynamics in proteins, polymers and other complex systems [1–6]. Experiments at variable magnetic field strength are also important for hyperpolarisation techniques, where they are used to determine relaxation rates and for polarisation transfer experiments [7–11].

Apparatus for NMR dispersion measurements fall into two categories; fast field-cycling methods where the sample remains in a static position whilst the magnetic field is swept [1–3,12–16], and sample shuttle methods where the sample is physically transported between regions with different magnetic field strength [8,17–28]. Sweeping the magnetic field using an electromagnet allows for very fast field-cycling (approximately 1 ms), however heating caused by the high electrical current required by the electromagnet limits the maximum field strength to around 2 T [1,12]. In contrast, sample shuttle methods are typically 1–2 orders of magnitude slower, with the fastest shuttles having transport times of 50 – 100 ms [6,18], but can access the higher magnetic fields and homogeneity offered by fixed strength magnets. Depending on the application, the low field environment in a sample shuttle system may either be a point within the stray field of the primary magnet, or a dedicated low field coil within a magnetic shield [25,28,29]. Combining a fixed strength magnet with magnet shielding elements and/or additional magnetic coils can allow extremely wide (9 orders of magnitude) magnetic field ranges to be studied on a single instrument [19,25].

Sample shuttles are either pneumatic or motor driven. Pneumatic systems are generally simpler to construct and offer fast transfer speeds [8,21–23,30], whereas motor driven systems offer a high degree of control over sample speed and position [17,20,25,27].

Whilst sample temperature control is common in fast field-cycling relaxometers [1,2,13], the difficulties in heating a moving sample mean that dispersion experiments on high field magnets using sample shuttles are usually carried out at room temperature or using a probe air heater [5,30]. Measurements at higher temperatures can be performed using a furnace to heat the air within the spectrometer bore [31]. Due to the low heat capacity of air, probe air heaters are not well suited to heating the sample at other points within the magnet bore, and can lead to significant temperature gradients [32,33]. In addition to altering relaxation rate, changes in sample temperature can cause convection within the sample, resulting in increased line broadening and reduced resolution.

We therefore propose a new design of sample shuttle that allows accurate control of sample temperature along with sample speed and position within the magnet stray field for use in NMR dispersion measurements.

2. Materials and methods

All experiments were performed on an Oxford Instruments wide bore 7.05 T magnet coupled to an Avance III Bruker NMR console. The instrument was equipped with a Bruker MIC5 microimaging probe fitted with a 10 mm $^{1}H/^{13}C$ resonator, an electrical probe

* Corresponding author.
E-mail address: G.Pileio@soton.ac.uk (G. Pileio).

https://doi.org/10.1016/j.jmr.2020.106778
1090-7807/

gas heating element and a 3-axis gradient system able to deliver pulsed field gradients of up to 1.5 T m^{-1}.

2.1. Sample preparation

2.1.1. $^{13}C_2$-Naphthalene-derivative (sample A)

1,2,3,4,5,6,8-heptakis([d_3]methoxy)-7-(([d_7]propan-2yl)oxy)-naphthalene-$^{13}C_2$ **1**, was synthesised according to the previously reported procedure [34]. 43.4 mg of **1** was dissolved in acetone d_6 (Sigma Aldrich 99.96%, 0.50 mL) to give a 0.2 M solution (sample A). The solution was filtered through a 0.2 μm syringe filter to remove any undissolved material before it was transferred to a 5 mm Young's tap NMR tube which had been freshly cleaned with a mixture of H_2O_2 and HCl to remove any paramagnetic impurities. The sample was degassed by ten freeze–pump-thaw cycles and was flame sealed to prevent oxygen or any other impurities from entering the NMR tube.

2.1.2. Maleate-derivative (sample B)

1-(ethyl-d_5),4-(propyl-d_7)(*Z*)-but-2-enedioate **2**, was synthesised according to the previously reported procedure [35]. 17 μL of **2** (16.6 mg) was dissolved in acetone d_6 (Sigma Aldrich 99.96%, 0.42 mL) to give a 0.2 M solution (sample B). The solution was transferred to a 5 mm Young's tap NMR tube which had been freshly cleaned with a mixture of H_2O_2 and HCl to remove any paramagnetic impurities. The sample was degassed by ten freeze–pump-thaw cycles and was flame sealed to prevent oxygen or any other impurities from entering the NMR tube.

2.2. Field map

Measurement of the magnetic field strength profile was carried out using a single-axis Hall effect sensor (Lakeshore 2Dex FA-251) mounted inside a standard 5 mm NMR tube. A PTFE spacer was used to position the sensor 20 mm above the base of the tube, in the centre of the probe coil region. The Hall sensor was supplied with a 2 mA constant current source, with the resultant voltage measured using a 16-bit analogue-to-digital converter (Adafruit ADS1115) and Arduino Uno board.

The tube and sensor were attached to the shuttle apparatus and positioned at full field within the probe. The shuttle motor was used to lift the sensor out of the magnet, with field strength measurements taken every 5 mm.

2.3. Temperature measurements

Sample temperature measurements were performed using 4-wire PT100 sensors (RS PRO 891–9148). For direct measurement of the sample temperature, two sensors were positioned 30 mm apart inside an NMR tube filled to 40 mm depth with deionised water (Fig. 6b). Temperature data was recorded using an Adafruit MAX31865 PT100 RTD temperature sensor amplifier and an Arduino Uno board.

Sample heating using the probe heater was carried out with a gas flow rate of 400 or 700 lph. After changing temperature, the sample was left to equilibrate for a minimum of 10 min before the next measurement.

2.4. Diffusion measurements

Diffusion measurements were performed on a sample of neat acetone-h_6 in either a 5 or 10 mm standard wall NMR tube using either a single (non-compensated) or double (convection compensated) stimulated echo pulse sequence. Bipolar gradients with magnitudes between 0.030 and 0.372 T m^{-1} and 2 ms duration ($\delta/2$) were used for diffusion measurement, with 0.05 s diffusion time (Δ). A single spoil gradient was used for non-compensated and three spoil gradients for compensated measurements. All spectra were recorded with a relaxation delay of 15 s and were processed with 1 Hz exponential line broadening.

Sample heating using the probe heater was carried out with a gas flow rate of 400 lph. After changing temperature, the sample was left to equilibrate for a minimum of 10 min before the next measurement.

2.4.1. T_1 Relaxation time measurements

T_1 relaxation measurements on sample A were carried out using a *pseudo*-2D T_1 inversion recovery pulse sequence modified to include trigger signals for the shuttle (Fig. 1a). The shuttle motor was operated in constant transport time mode with a transport time τ_t = 4 s and a positioning delay τ_p = 0.5 s introduced to ensure that the sample had stopped moving before the detection pulse was applied. Measurements were taken with variable delays τ_R of 10, 30, 50, 90, 120, 200, 300 and 500 s for each temperature and field. A 500 s relaxation delay was used to allow magnetisation to reach thermal equilibrium. Spectra were processed with 1 Hz line broadening and integrated.

2.4.2. T_s relaxation time measurements

Singlet state relaxation measurements were carried out using a *pseudo*-2D M2S-S2M pulse sequence[26] modified to include trigger signals for the shuttle motor (Fig. 1b). A Spin Lock Induced Coupling (SLIC) pulse[33] followed by a T_{00} filter block were repeated n_3 = 5 times to remove any residual singlet order before the start of the experiment. The duration of the gradients in the T_{00} filter was set to 2.4 ms, 1.2 ms and 1.2 ms for G_1, G_2 and G_3, respectively. Their strength was set to 45 mT m^{-1}, −45 mT m^{-1} and −60 mT m^{-1}, respectively. Delays and other parameters were optimised experimentally for the sample and spectrometer to maximise magnetisation to singlet order conversion efficiency.

For sample A, a relaxation delay of 300 s and SLIC pulse duration of 1 s were used. The M2S-S2M parameters were optimised to n_1 = 20, n_2 = 10 and τ_e = 9.14 ms. The shuttle motor was operated in constant transport time mode with τ_t = 4 s and τ_p = 0.5 s. Measurements were taken with variable delays τ_R of 90, 180, 370, 720, 1440, 2880, 5760 and 11520 s for each temperature and field, and fitted to an exponential decay function. Spectra were processed with 1 Hz line broadening and integrated.

For sample B, a relaxation delay of 100 and SLIC pulse duration of 1 s were used. The M2S-S2M parameters were optimised to n_1 = 20, n_2 = 10 and τ_e = 41.8 ms The shuttle motor was operated in constant transport time mode with τ_t = 3.5 s and τ_p = 0.5 s. Measurements were taken with variable delays τ_R of 10, 20, 40, 60, 80, 120, 160, 240, 480, 920 and 184 s for each temperature and field, and fitted to an exponential decay function. Spectra were processed with 3 Hz line broadening and integrated. No water suppression was required for this experiment due to the long relaxation time of the singlet order and the T_{00} filter which removed any residual magnetisation prior to conversion and detection of the singlet order.

3. Hardware design

The sample shuttle (Fig. 2) was designed to be compatible with a Bruker 300 MHz spectrometer to allow variable-temperature NMR dispersion measurements to be made using the stray field of the 7 T wide bore magnet. The apparatus consisted of three parts: an acrylic plastic shuttle containing the sample and heat transfer fluid (a mixture of water and ethylene glycol), a stepper motor, and a guide tube.

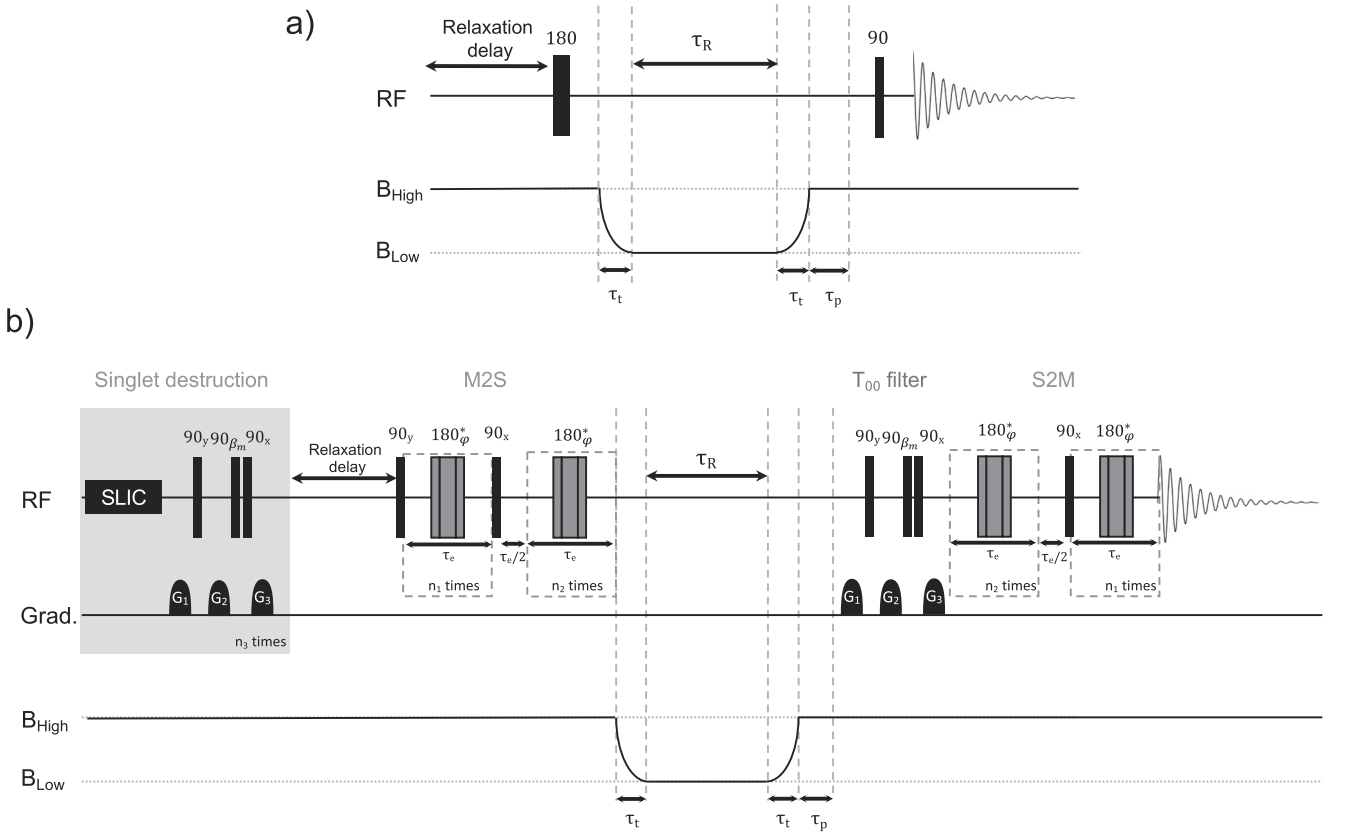

Fig. 1. a) Schematic of modified inversion recovery pulse sequence used for T_1 relaxation time measurements, showing the relative position of the sample within the magnet stray field. b) Schematic of M2S-S2M pulse sequence used for singlet state relaxation measurements, showing the relative position of the sample within the magnet stray field. M2S = magnetisation to singlet transfer, S2M = singlet to magnetisation transfer, τ_R = variable relaxation delay at low field, τ_t = transport time, τ_p = positioning delay, G_n = gradient pulse, SLIC = Spin Lock Induced Coupling pulse [33], $n_1 = \pi J/(2\Delta\nu)$, $n_2 = n_1/2$. $\tau_e = 1/\left(2\sqrt{J^2+\Delta\nu^2}\right)$, β_m = 54.74, 180^*_φ = composite 180° pulse comprising of $[90_{90}°240_0°\ 90_{90}°]_\varphi$ with φ cycled through the n_1 and n_2 repetitions as [x, x,-x,-x, -x, x, x, -x, -x, -x, x, x, -x, -x, x]. J is the value of the scalar coupling between the two spins in the singlet pair and $\Delta\nu$ their difference in chemical shift frequency.

3.1. Sample shuttle

The sample shuttle body was constructed from acrylic tube (31 mm OD, 26 mm ID, 180 mm length). A sample holder custom 3D-printed from nylon (Figure S7 in supporting information) was designed to hold a sample tube in a standard Bruker spinner at the correct depth within the probe. Two O-rings on the outside of the sample holder provided a tight compression fitting to the sample shuttle body, preventing the heat transfer fluid from leaking whilst maintaining easy access to change the sample. An end cap machined from polyoxymethylene prevented leaks from the top of the shuttle and provided a fixture for the winch cord and temperature sensor.

Heat transfer fluid entered from the bottom of the shuttle through a rigid acrylic tube (10 mm OD, 7 mm ID, 1 m length), which extended through the probe to the bottom of the spectrometer, sliding freely as the shuttle is raised and lowered. The heat transfer fluid flowed up through channels in the sample holder and around the sample, filling the body of the sample shuttle, before exiting via a flexible PVC hose (8 mm OD, 6 mm ID) connected to the top of the sample shuttle (Fig. 3).

3.2. Guide tube

The entire shuttle assembly was free to move vertically along a guide tube constructed of rigid acrylic tube (38 mm OD, 32 mm ID). The guide tube extended one metre up from the top of the probe and ensured that the shuttle remained concentric with the magnet bore (Fig. 3). Nylon spacer rings (72 mm OD, 38 mm ID, 10 mm thickness) were used to support the guide tube within the magnet bore.

3.3. Stepper motor

A Trinamic TMCL-1160 stepper motor located outside of the stray field of the magnet was used to lift the sample out of the magnet when a trigger signal was received from the spectrometer console. Due to restricted ceiling height it was not possible to position the stepper motor directly above the magnet. High tensile strength Dynema cord with a low stretch ratio was attached to the top of the sample shuttle and connected to the motor via a pulley mounted above the spectrometer and a custom 25 cm diameter spindle wheel 3D printed from ABS plastic. Adaptation to a gear driven system for use on other magnets would require only minor modification.

A custom printed circuit board was used to supply power to the motor driver and to amplify the trigger outputs from the spectrometer console at 5 V to the 10 V needed for the motor hardware. A light gate positioned at the top of the shuttle guide tube was used to cut power to the motor to prevent the sample exiting the guide tube in case of malfunction but was not otherwise used to determine sample position.

3.4. Control of shuttle position and speed

Position and timing of the shuttle was controlled by the spectrometer computer using Python scripts integrated with the acqui-

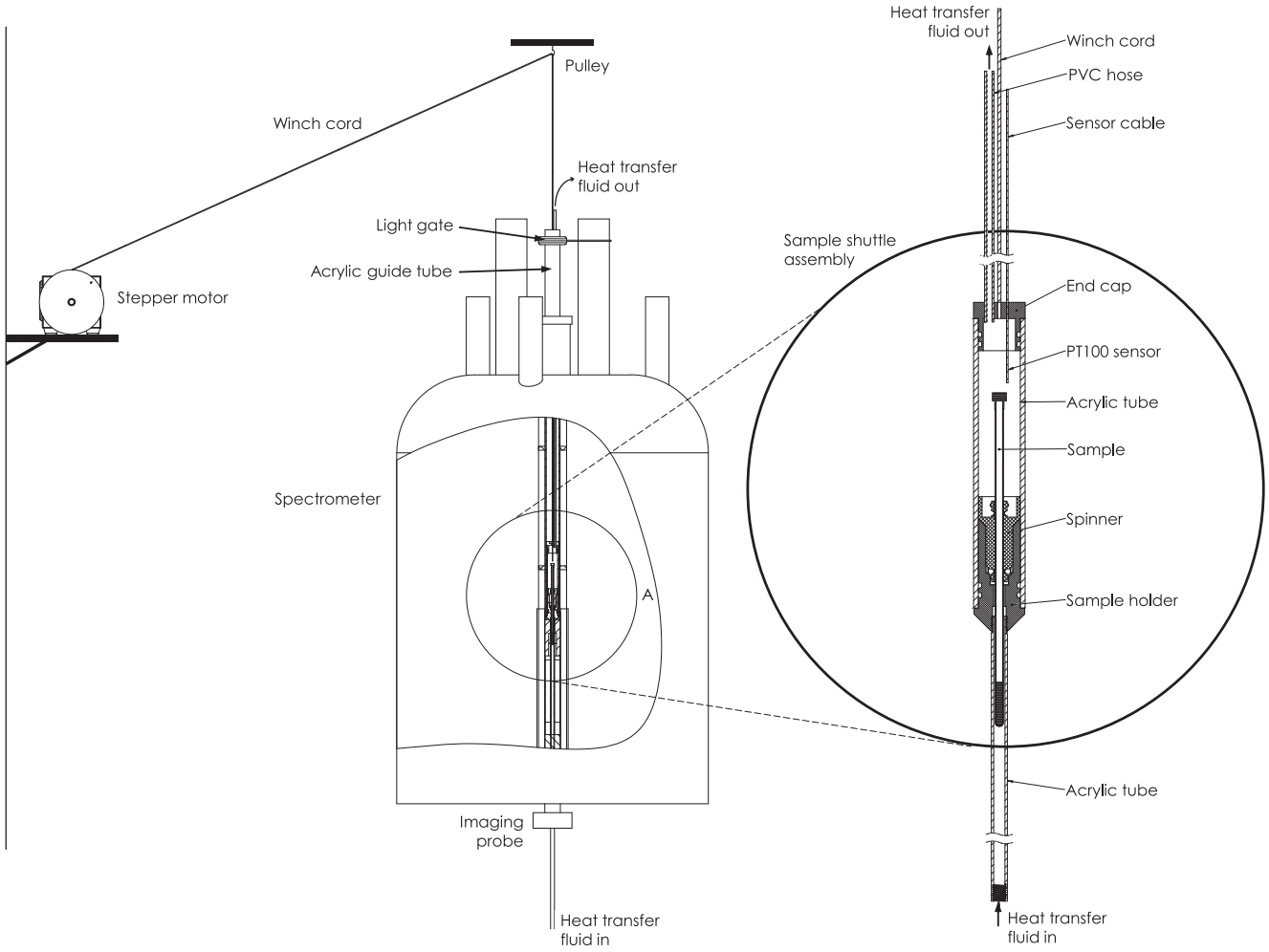

Fig. 2. Schematic of the temperature-controlled sample shuttle apparatus.

sition software. Prior to acquisition, constants set in the TopSpin acquisition window relating to speed, acceleration and target field strength were read by the Python scripts and stored in the motor memory. During acquisition, TTL signals from the spectrometer console were used to trigger the motor to move up or down at times specified in the pulse program.

The magnetic field profile of the spectrometer (Fig. 4) was determined experimentally using a miniature Hall effect sensor within an NMR tube. The measured field map was used to calculate the position to which the shuttle should be moved for any arbitrary field strength within the range of the instrument as specified by the user.

The speed and acceleration ramp of the motor were set as constants within the TopSpin acquisition program and relayed to the motor via the Python scripts. Depending on application, the motor could be set to either maintain a constant speed (with the transport time proportional to the distance moved by the shuttle), a constant transport time or to follow a velocity profile that varied as a function of position/field. The latter feature allowed for adiabatic and other field profiles during transport of the sample between high and low field regions.

Although transport speeds of up to 1.2 m.s^{-1} were theoretically possible, we chose to limit experiments to a maximum of 0.25 m.s^{-1} (corresponding to a transport time of around 2.5 s to reach 50 mT) to avoid damage to the motor due to the increased torque required to lift the heavier shuttle. Whilst not as fast as some rapid shuttle systems [6,18], this was still adequate to measure relaxation times of many molecules.

3.5. Temperature control

Temperature control in commercial NMR probes relies on an inert carrier gas – typically nitrogen – to act as a heat transfer medium. The gas is either preheated/cooled before entering the probe or is heated using an electrical heating element inside the probe. The gas then flows around the sample before exiting the magnet either through the magnet bore or via dedicated channels.

Since the sample is heated from the bottom of the tube, this may cause temperature gradients in the sample, leading to convection. Convection in NMR samples is a well-known problem, particularly for low viscosity solvents, and has led to many solutions to minimise convection including restricted volume tubes [36] and convection compensated pulse sequences [37–40].

Due to the low heat capacity of nitrogen, high flow rates (typically 400 – 800 lph) are required to maintain sample temperature. Heat losses to the surroundings means that temperature drops as the distance from the probe heater increases. Whilst not normally a problem for samples remaining in a fixed position in the probe, this presents a major challenge for stray field measurements at temperatures above or below ambient.

Temperature control in the sample shuttle was achieved using a Julabo DYNEO DD-200F recirculating heater/chiller filled with a 9:1

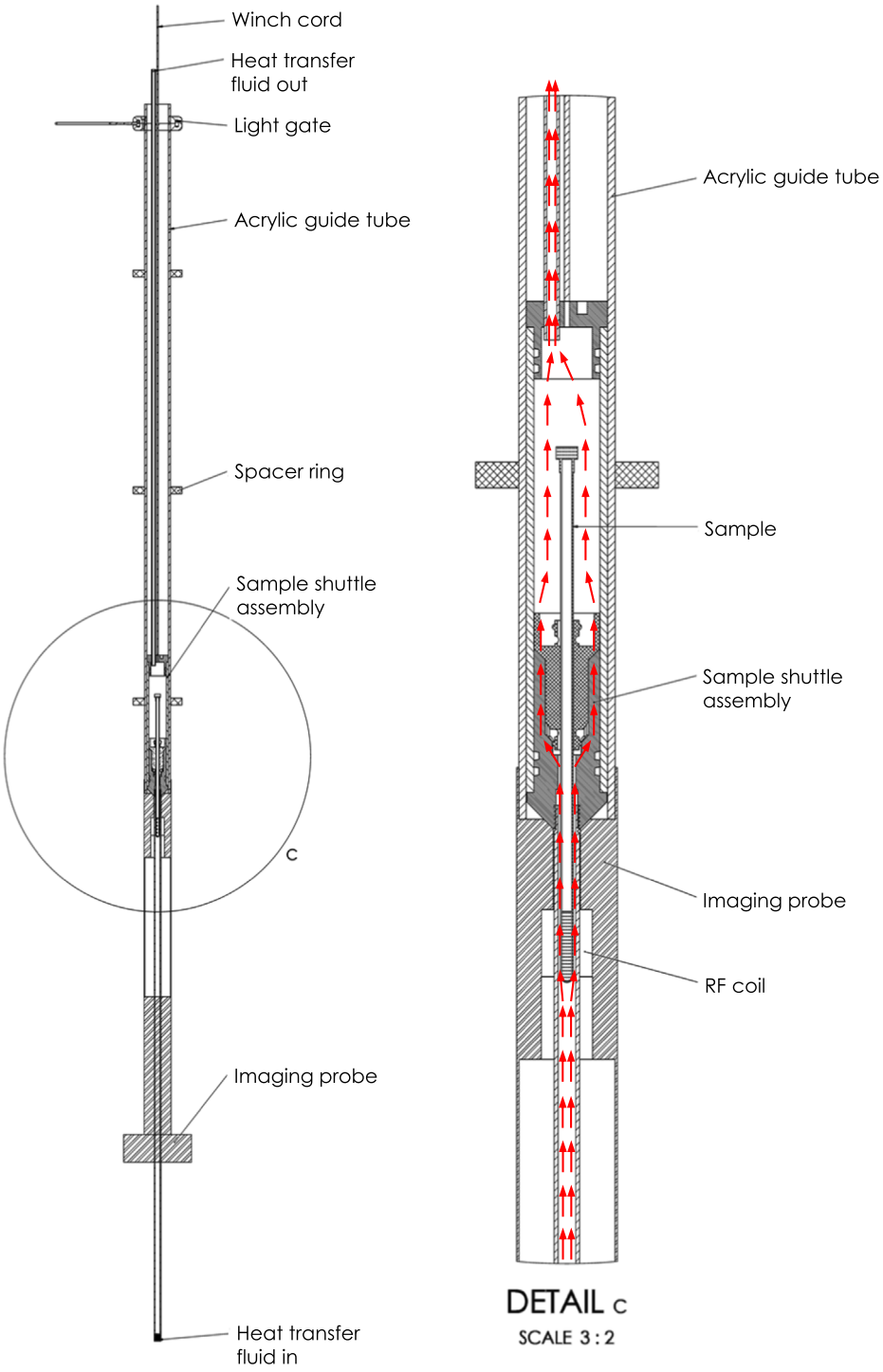

Fig. 3. Schematic of the temperature-controlled sample shuttle and guide tube. Red arrows indicate the flow path of the heat transfer fluid.

water/ethylene glycol mixture. The heat transfer fluid mixture flowed around the inside of the sample shuttle, surrounding the sample to maintain a constant temperature bath. The temperature of the heater/chiller water bath was set with respect to an external temperature probe (PT100) positioned inside the sample shuttle. The much higher heat capacity of water compared to nitrogen meant that a constant temperature could be maintained across the entire sample, with temperature gradients < 0.05 °C (Table 1).

4. Results and discussion

To investigate temperature gradients resulting from sample heating, two PT100 temperature sensors were positioned inside a 5 mm sample tube containing water (Fig. 5a). Without sample heating or gas flow both temperature sensors gave a reading within ± 0.2 °C of the ambient temperature (20.7 °C). Heating to 25 °C using the probe air heater resulted in a 1.5 °C difference between the two sensors. (Note: These measurements were per-

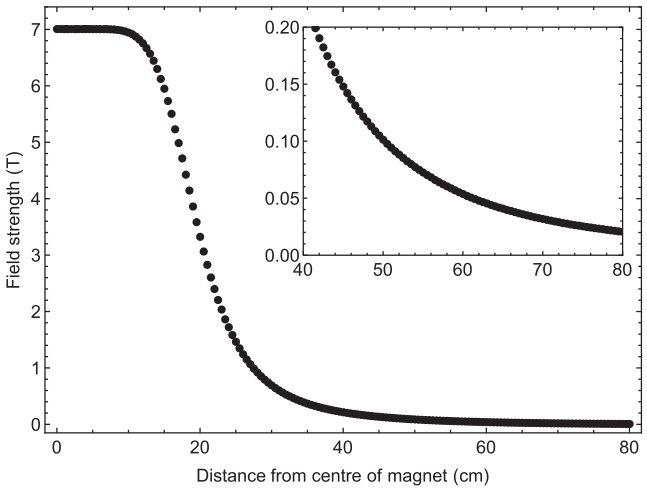

Fig. 4. Experimentally measured field map of the 7 T magnet used for field-cycling experiments, showing variation in B_0 magnetic field along the magnet bore. INSET: Expansion of 0 – 0.2 T region.

formed using a 10 mm MRI probe with an electrical heating element. Temperature gradients of between 0.05 and 1.65 K.cm^{-1} have also been observed on a modern solution state spectrometers fitted with room temperature or cryoprobes [32,33].) Increasing the gas flow rate improved heating of the sample but did not improve the temperature gradient across the sample. Increasing the temperature to 40 °C led to an even greater difference between the two sensors at both flow rates.

The effect of the temperature gradient on sample convection can be clearly seen in DOSY measurements on a sample of acetone-h_6 (Fig. 5b). Without sample heating a normal Gaussian dependence on gradient strength was observed. Heating the sample to just 4 °C above ambient resulted in large distortions that are associated with sample convection [40], caused by the 1.5 °C difference in temperature measured between the top and bottom of the sample. Convection effects resulted in a vast overestimation of the diffusion constant, accompanied by large fitting errors (Fig. 5c).

Using a double stimulated echo pulse sequence (convection compensated) allowed the effects of sample convection to be removed from the spectra, producing good quality data even at higher temperatures (Fig. 5). Despite removing convection artefacts from the measured spectra, this pulse sequence cannot prevent the underlying physical process causing the distortions and so convection issues may still arise in other processes such as altered relaxation rates [33].

The high heat capacity of water meant that the temperature gradient was much smaller when using the sample shuttle than the probe heater, effectively eliminating convection in the sample. Eliminating convection resulted in normal Gaussian diffusion plots, even without the use of convection compensated pulse sequences (Fig. 5).

A challenge of using water as a heat transfer medium was that the water was observable in the proton NMR spectrum of the sample, since the water had to travel through the active region of the probe. This problem was alleviated somewhat by the flow of the water, as if the flow rate was fast enough water entering the probe region did not have time to build up full magnetisation, reducing the observed signal.

Selective excitation of the sample peak was also found to be an effective way of suppressing the water signal, providing that the sample peaks were sufficiently distant from the water resonance (Figure S2 in the supporting information). If the relaxation time of the sample was long compared to that of water (or the rate at which the water is flowing through the coil region) then no suppression was required since the water signal had relaxed before the spectrum was detected.

For other nuclei (with the exception of ^{17}O), water is an ideal heat transfer medium since it results in no additional signal in the spectrum. Substitution of water for a polyfluorinated oil may offer an alternative heat transfer medium with no proton signal, however this has yet to be tested.

To demonstrate the application of the sample shuttle for NMR dispersion measurements at variable temperature, we have measured the T_1 and singlet order relaxation time (T_S) of the doubly carbon-13 labelled naphthalene derivative, **1** (Scheme 1). This molecule was designed to support a long-lived singlet state on the two adjacent ^{13}C nuclei whilst minimising intramolecular relaxation pathways [34]. Previous studies at fixed temperature have shown that a maximum T_S relaxation time of 4250 ± 130 s can be achieved for this molecule at a field strength of 0.4 T [41].

The long delays required for relaxation measurements makes them particularly susceptible to even small amounts of convection, which results in a faster apparent relaxation rate due to transport of sample out of the active volume [33]. Relaxation measurements are therefore ideally suited to the sample shuttle and the improved temperature control compared to air heated probes.

Singlet order was generated from thermal magnetisation using a magnetisation-to-singlet (M2S) spin-echo train and was allowed to evolve for a variable time before it was reconverted to observable magnetisation through an S2M sequence immediately before acquisition (Fig. 1) [26]. During the variable time delay between the two spin-echo trains, the sample was transported to a point within the stray field of the magnet, where it was held for a relaxation time period, τ_R, before being returned to the probe. By varying τ_R and fitting the resultant *pseudo*-2D spectrum using an exponential decay function, the singlet order relaxation time constant, T_S, was determined for relaxation field strengths between 0.050 and 7.056 T and temperatures between 283 and 303 K (Fig. 6a & b). T_1 relaxation time (Fig. 6c & d) was also measured on the same sample using a conventional inversion-recovery experiment.

Singlet relaxation times of sample A showed strong temperature and field dependencies (Fig. 6a & b). The interaction of different relaxation mechanisms as a function of temperature and field strength is complex, however the results at 293 K are consistent

Table 1
Comparison of temperature gradient across the sample tube with different heating methods. Uncertainty in sensor measurements represents tolerance within temperature range (class A).

Entry	Heating method	Gas flow (lph)	Target temperature (°C)	Sensor 1 (°C) ± 0.20 °C	Sensor 2 (°C) ±0.20 °C	Difference (°C)
1	None	0	–	20.66	20.53	0.13
2	Probe heater	400	25	21.31	22.86	1.55
3	Probe heater	700	25	21.78	23.40	1.62
4	Probe heater	400	40	25.06	31.25	6.19
5	Probe heater	700	40	27.12	33.59	6.47
6	Sample shuttle	–	25	24.65	24.69	0.04
7	Sample shuttle	–	40	39.70	39.70	0.00

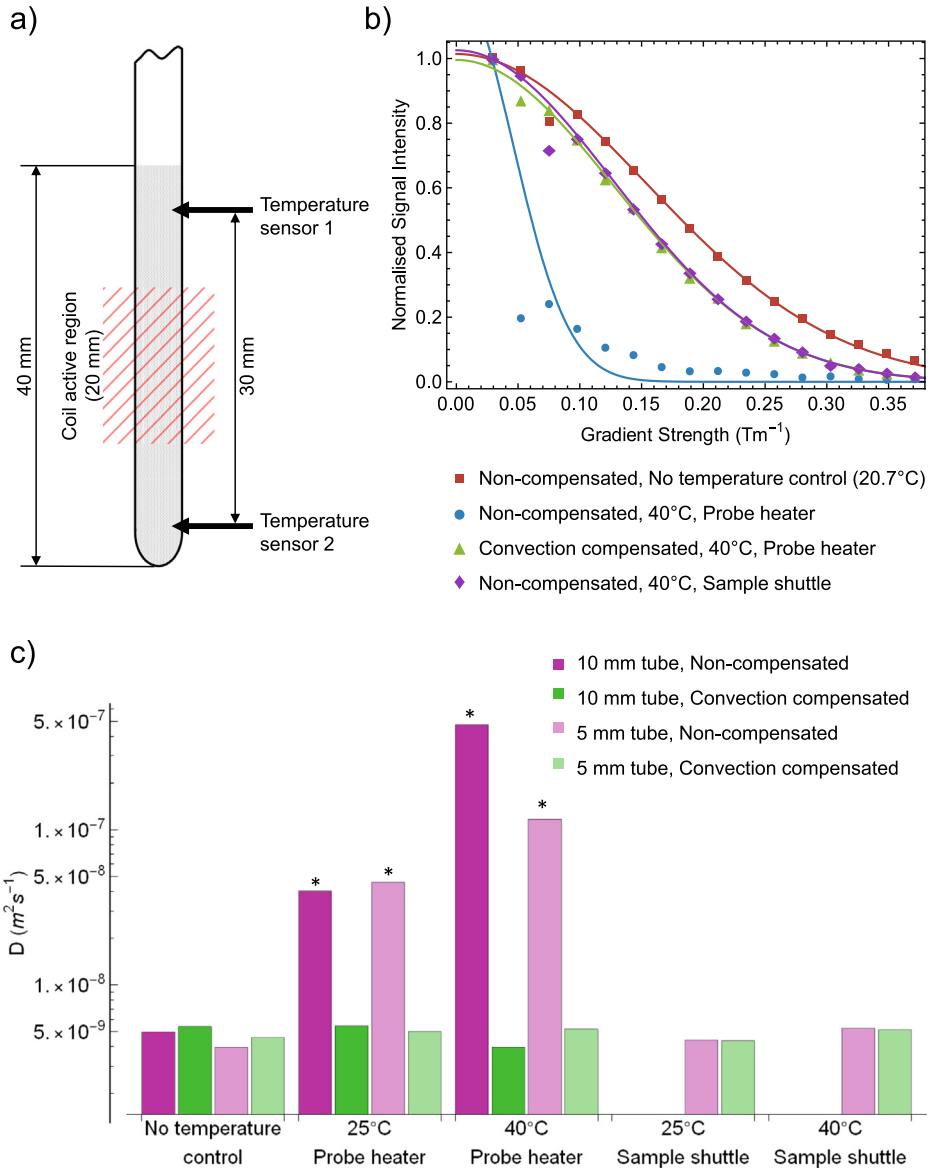

Fig. 5. a) Schematic of experimental set-up for temperature sensor measurements. b) Comparison of pulsed gradient diffusion measurements with different sample heating methods, with and without convection compensated pulse sequences (neat acetone-h_6 in a 5 mm NMR tube). c) Diffusion constants measured with and without convection compensated pulse sequences in tubes of different diameters and using different sample heating methods on a sample of neat acetone-h_6. * Very large fitting errors are associated with these measurements.

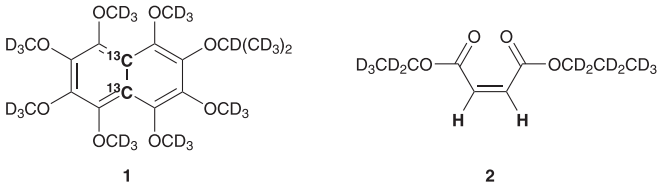

Scheme 1. Structures of the isotopically labelled derivative of naphthalene **(1)** and the asymmetric maleate diester **(2)** used in this paper.

with previously reported measurements where Chemical Shift Anisotropy (CSA) was found to dominate at higher fields and Spin Internal Motion (SIM) at lower fields [41]. The relaxation rate was found to be lowest at 303 K and a field strength of 0.25 T, with a new record T_s lifetime for this molecule of 6480 ± 830 s.

A similar trend with respect to magnetic field strength was observed for the T_1 relaxation time of sample A, however the effect of temperature was less pronounced (Fig. 6c). The dip in the T_1 relaxation time data observed between 0.1 and 0.5 T (Fig. 6d) and its dependence on temperature is here highlighted but is beyond the scope of this paper and was not investigated further.

In a second demonstration of the proposed equipment, we measure the relaxation time of singlet order as a function of the temperature in the asymmetrically substituted maleate derivative (sample B). Asymmetric maleates are of interest due to their ability to form singlet order with relaxation lifetimes several times that of the triplet state [33,42]. Whilst singlet lifetimes of maleates are typically an order of magnitude lower than those of the naphthalene derivative, maleates are readily formed by hydrogenation of the corresponding acetylene diester and are therefore ideal model compounds for investigating storage of hyperpolarisation generated from *para*-hydrogen [43].

Fig. 7 shows the values of T_S measured at different sample temperatures between 278 and 323 K for a sample of *n*-propyl ethyl maleate, **2** (Scheme 1) using our temperature-controlled sample

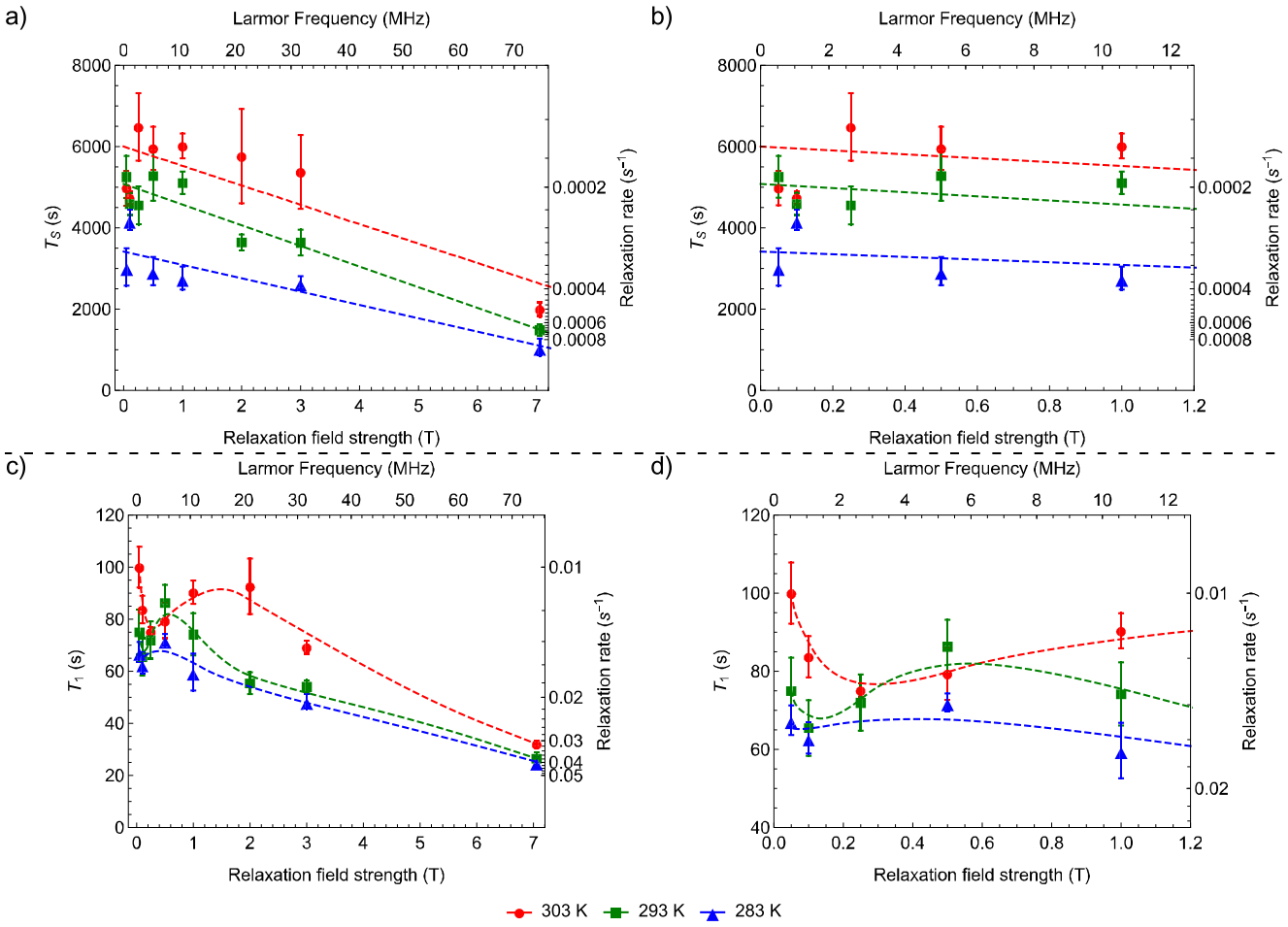

Fig. 6. a) Variation in singlet order relaxation time decay constant as a function of relaxation field strength and temperature for sample A. Dashed lines indicate the line of best fit; b) Expansion of the 0 – 1 T region of the T_s data in a); c) Variation in T_1 relaxation time decay constant as a function of relaxation field strength and temperature for sample A. Dashed lines indicate a smoothed moving average of the data. d) Expansion of the 0 – 1 T region of the T_1 data in c). Error bars indicate uncertainty from the fitting. (Red circles = 303 K, Green squares = 293 K, Blue triangles = 283 K).

shuttle. The data revealed a very strong temperature dependence, with faster relaxation occurring at lower temperatures. A T_s value of 682 ± 62 s as found at 40 °C constitutes a gain of >25% with respect to the value found at room temperature (544 ± 16 s), highlighting the importance of temperature in the relaxation mechanisms of long-lived states and its role as a valuable variable to be used in order to prolong the storage of hyperpolarised magnetisation.

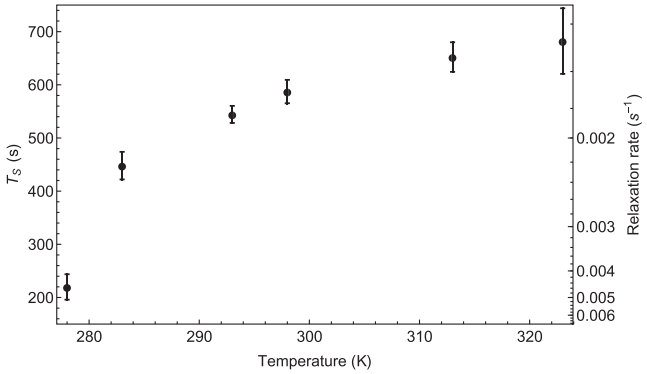

Fig. 7. Variation in singlet order relaxation time decay constant as a function of temperature for sample B at a constant field strength of 7 T. Error bars indicate uncertainty from fitting relaxation data.

5. Conclusions

We have demonstrated a design for a new temperature-controlled sample shuttle for NMR dispersion measurements. The shuttle and control software allowed the sample to be transported to any point within the stray field of the magnet in a controlled and reproducible manner. Water was used as a heat transfer medium to regulate the temperature of the sample independently of position within the magnet bore and with a variation of <0.05 K across the sample.

Using the sample shuttle, we have shown how the T_1 and singlet order relaxation decay constants of two custom-made singlet-bearing molecules varies with temperature and magnetic field strength. In both examples, a strong dependence on magnetic field strength and temperature was observed, with record breaking singlet lifetimes measured for both molecules at above ambient temperature.

In addition to investigation of relaxation mechanisms, this apparatus is particularly useful in minimising thermal convection in diffusion-NMR experiments and for the study of molecular dynamics, which often exhibit strong temperature dependences. More generally, it offers the possibility to run any experiments at constant (or variable) field strength where greater temperature accuracy is required than can be provided by conventional probe air heaters.

CRediT authorship contribution statement

Andrew M.R. Hall: Methodology, Software, Investigation, Formal analysis, Writing - original draft. **Topaz A.A. Cartlidge:** Investigation, Formal analysis. **Giuseppe Pileio:** Conceptualization, Methodology, Supervision, Validation, Funding acquisition, Writing - review & editing.

Acknowledgements

This work was supported by a research grant from EPSRC, United Kingdom (EP/P005187/1) "HyperStore: Singlet states and supercritical fluids for storage and transport of hyperpolarised spin order". The authors would like to thank LakeShore Cryotonics for supplying the miniature Hall effect sensor used for magnetic field strength measurements, Dr Lynda Brown for synthesis of labelled compounds and Dr Francesco Giustiniano for many useful discussions. The authors acknowledge the COST, European Union, CA15209 ‘‘, "European Network on NMR Relaxometry".

Conflict of Interest

The authors declare no conflicts of interest.

Appendix A. Supplementary data

Supplementary data to this article can be found online at https://doi.org/10.1016/j.jmr.2020.106778.

References

[1] R. Kimmich, Field-Cycling NMR Relaxometry: Instrumentation, Model Theories and Applications; Kimmich, R., Ed.; Royal Society of, Chemistry (2018) 358–384, https://doi.org/10.1039/9781788012966.
[2] E. Anoardo, G. Galli, G. Ferrante, Fast-Field-Cycling NMR: Applications and Instrumentation, Appl. Magn. Reson. 20 (3) (2001) 365–404, https://doi.org/10.1007/BF03162287.
[3] R.M. Steele, J.-P. Korb, G. Ferrante, S. Bubici, New Applications and Perspectives of Fast Field Cycling NMR Relaxometry, Magn. Reson. Chem. 54 (6) (2016) 502–509, https://doi.org/10.1002/mrc.4220.
[4] M. Flämig, M. Hofmann, A. Lichtinger, E.A. Rössler, Application of Proton Field-Cycling NMR Relaxometry for Studying Translational Diffusion in Simple Liquids and Polymer Melts, Magn. Reson. Chem. 57 (10) (2019) 805–817, https://doi.org/10.1002/mrc.4823.
[5] Cousin, S. F.; Kadeřávek, P.; Bolik-Coulon, N.; Ferrage, F. Determination of Protein Ps-Ns Motions by High-Resolution Relaxometry. In Methods in Molecular Biology: Protein NMR; Ghose, R., Ed.; Humana Press Inc.: New York, 2018; Vol. 1688, pp 169–203. https://doi.org/10.1007/978-1-4939-7386-6_9.
[6] C. Charlier, S.N. Khan, T. Marquardsen, P. Pelupessy, V. Reiss, D. Sakellariou, G. Bodenhausen, F. Engelke, F. Ferrage, Nanosecond Time Scale Motions in Proteins Revealed by High-Resolution Nmr Relaxometry, J. Am. Chem. Soc. 135 (49) (2013) 18665–18672, https://doi.org/10.1021/ja409820g.
[7] A.S. Kiryutin, A.N. Pravdivtsev, K.L. Ivanov, Y.A. Grishin, H.-M. Vieth, A.V. Yurkovskaya, A Fast Field-Cycling Device for High-Resolution NMR: Design and Application to Spin Relaxation and Hyperpolarization Experiments, J. Magn. Reson. 263 (2016) 79–91, https://doi.org/10.1016/j.jmr.2015.11.017.
[8] P. TomHon, E. Akeroyd, S. Lehmkuhl, E.Y. Chekmenev, T. Theis, Automated Pneumatic Shuttle for Magnetic Field Cycling and Parahydrogen Hyperpolarized Multidimensional NMR, J. Magn. Reson. 312 (2020), https://doi.org/10.1016/j.jmr.2020.106700.
[9] A. Krahn, P. Lottmann, T. Marquardsen, A. Tavernier, M.T. Türke, M. Reese, A. Leonov, M. Bennati, P. Hoefer, F. Engelke, C. Griesinger, Shuttle DNP Spectrometer with a Two-Center Magnet, Phys. Chem. Chem. Phys. 12 (22) (2010) 5830–5840, https://doi.org/10.1039/c003381b.
[10] J. Natterer, J. Bargon, Parahydrogen Induced Polarization, Prog. Nucl. Magn. Reson. Spectrosc. 31 (4) (1997) 293–315, https://doi.org/10.1016/S0079-6565(97)00007-1.
[11] M.H. Levitt, Long Live the Singlet State!, J. Magn. Reson. 306 (2019) 69–74, https://doi.org/10.1016/j.jmr.2019.07.029.
[12] R. Kimmich, E. Anoardo, Field-Cycling NMR Relaxometry, Prog. Nucl. Magn. Reson. Spectrosc. 44 (2004) 257–320, https://doi.org/10.1016/j.pnmrs.2004.03.002.
[13] M. Bödenler, L. de Rochefort, P.J. Ross, N. Chanet, G. Guillot, G.R. Davies, C. Gösweiner, H. Scharfetter, D.J. Lurie, L.M. Broche, Comparison of Fast Field-Cycling Magnetic Resonance Imaging Methods and Future Perspectives, Mol. Phys. 117 (7–8) (2019) 832–848, https://doi.org/10.1080/00268976.2018.1557349.
[14] G. Ferrante, S. Sykora, Technical Aspects of Fast Field Cycling. In Advances in Inorganic, Chemistry; Academic Press Inc., 2005, pp. 405–470, https://doi.org/10.1016/S0898-8838(05)57009-0.
[15] C. Job, J. Zajicek, M.F. Brown, Fast Field-Cycling Nuclear Magnetic Resonance Spectrometer, Rev. Sci. Instrum. 67 (1996) 2113, https://doi.org/10.1063/1.1147024.
[16] F. Noack, NMR Field-Cycling Spectroscopy: Principles and Applications, Prog. Nucl. Magn. Reson. Spectrosc. 18 (3) (1986) 171–276, https://doi.org/10.1016/0079-6565(86)80004-8.
[17] A.G. Redfield, High-Resolution NMR Field-Cycling Device for Full-Range Relaxation and Structural Studies of Biopolymers on a Shared Commercial Instrument, J. Biomol. NMR 52 (2) (2012) 159–177, https://doi.org/10.1007/s10858-011-9594-1.
[18] C.Y. Chou, M. Chu, C.F. Chang, T.H. Huang, A Compact High-Speed Mechanical Sample Shuttle for Field-Dependent High-Resolution Solution NMR, J. Magn. Reson. 214 (2012) 302–308, https://doi.org/10.1016/j.jmr.2011.12.001.
[19] C.-Y. Chou, F. Ferrage, G. Aubert, D. Sakellariou, Simple Method for the Generation of Multiple Homogeneous Field Volumes inside the Bore of Superconducting Magnets, Sci. Rep. 5 (1) (2015) 12200, https://doi.org/10.1038/srep12200.
[20] C.Y. Chou, M. Chu, C.F. Chang, T. Yu, T. Huang, Huang, D. Sakellariou, High Sensitivity High-Resolution Full Range Relaxometry Using a Fast Mechanical Sample Shuttling Device and a Cryo-Probe, J. Biomol. NMR 66 (3) (2016) 187–194, https://doi.org/10.1007/s10858-016-0066-5.
[21] S.F. Cousin, C. Charlier, P. Kadeřávek, T. Marquardsen, J.M. Tyburn, P.A. Bovier, S. Ulzega, T. Speck, D. Wilhelm, F. Engelke, W. Maas, D. Sakellariou, G. Bodenhausen, P. Pelupessy, F. Ferrage, High-Resolution Two-Field Nuclear Magnetic Resonance Spectroscopy, Phys. Chem. Chem. Phys. 18 (48) (2016) 33187–33194, https://doi.org/10.1039/c6cp05422f.
[22] S.D. Swanson, S.D. Kennedy, A Sample-Shuttle Nuclear-Magnetic-Relaxation-Dispersion Spectrometer, J. Magn. Reson. - Ser. A 102 (3) (1993) 375–377, https://doi.org/10.1006/jmra.1993.1121.
[23] V. Biancalana, Y. Dancheva, L. Stiaccini, Note: A Fast Pneumatic Sample-Shuttle with Attenuated Shocks, Rev. Sci. Instrum. 85 (3) (2014), https://doi.org/10.1063/1.4868092.
[24] D. Wu, C.S. Johnson, Diffusion-Ordered 2D NMR in the Fringe Field of a Superconducting Magnet, J. Magn. Reson. Ser. A 116 (2) (1995) 270–272, https://doi.org/10.1006/jmra.1995.0020.
[25] I.V. Zhukov, A.S. Kiryutin, A.V. Yurkovskaya, Y.A. Grishin, H.M. Vieth, K.L. Ivanov, Field-Cycling NMR Experiments in an Ultra-Wide Magnetic Field Range: Relaxation and Coherent Polarization Transfer, Phys. Chem. Chem. Phys. 20 (18) (2018) 12396–12405, https://doi.org/10.1039/c7cp08529j.
[26] G. Pileio, M. Carravetta, M.H. Levitt, Storage of Nuclear Magnetization as Long-Lived Singlet Order in Low Magnetic Field, Proc. Natl. Acad. Sci. 107 (40) (2010) 17135–17139, https://doi.org/10.1073/PNAS.1010570107.
[27] Huang, T.-H.; Chou, C.-Y.; Chu, M.-L.; Chang, C.-F. High Speed Sample Transportation Apparatus in a Superconducting Magnet and Transporting Method Thereof. US9696391B2, May 6, 2012.
[28] C.-Y. Chou, M. Abdesselem, C. Bouzigues, M. Chu, A. Guiga, T.-H. Huang, F. Ferrage, T. Gacoin, A. Alexandrou, D. Sakellariou, Ultra-Wide Range Field-Dependent Measurements of the Relaxivity of Gd1−xEuxVO4 Nanoparticle Contrast Agents Using a Mechanical Sample-Shuttling Relaxometer, Sci. Rep. 7 (1) (2017) 44770, https://doi.org/10.1038/srep44770.
[29] P.J. Ganssle, H.D. Shin, S.J. Seltzer, V.S. Bajaj, M.P. Ledbetter, D. Budker, S. Knappe, J. Kitching, A. Pines, Ultra-Low-Field NMR Relaxation and Diffusion Measurements Using an Optical Magnetometer, Angew. Chemie Int. Ed. 53 (37) (2014) 9766–9770, https://doi.org/10.1002/anie.201403416.
[30] A.G. Redfield, Shuttling Device for High-Resolution Measurements of Relaxation and Related Phenomena in Solution at Low Field, Using a Shared Commercial 500 MHz NMR Instrument, Magn. Reson. Chem. 41 (10) (2003) 753–768, https://doi.org/10.1002/mrc.1264.
[31] H. Stork, M. Ditter, H. Plößer, A.F. Privalov, F. Fujara, High Temperature Mechanical Field-Cycling Setup, J. Magn. Reson. 192 (2) (2008) 173–176, https://doi.org/10.1016/j.jmr.2008.02.017.
[32] N.M. Loening, J. Keeler, Temperature Accuracy and Temperature Gradients in Solution-State NMR Spectrometers, J. Magn. Reson. 159 (1) (2002) 55–61, https://doi.org/10.1016/S1090-7807(02)00120-9.
[33] B. Kharkov, X. Duan, J.W. Canary, A. Jerschow, Effect of Convection and B1 Inhomogeneity on Singlet Relaxation Experiments, J. Magn. Reson. 284 (2017) 1–7, https://doi.org/10.1016/j.jmr.2017.09.005.
[34] J.T. Hill-Cousins, I.A. Pop, G. Pileio, G. Stevanato, P. Håkansson, S.S. Roy, M.H. Levitt, L.J. Brown, R.C.D. Brown, Synthesis of an Isotopically Labeled Naphthalene Derivative That Supports a Long-Lived Nuclear Singlet State, Org. Lett. 17 (9) (2015) 2150–2153, https://doi.org/10.1021/acs.orglett.5b00744.
[35] J.-N. Dumez, J.T. Hill-Cousins, R.C.D. Brown, G. Pileio, Long-Lived Localization in Magnetic Resonance Imaging, J. Magn. Reson. 246 (2014) 27–30, https://doi.org/10.1016/j.jmr.2014.06.008.

[36] I. Swan, M. Reid, P.W.A. Howe, M.A. Connell, M. Nilsson, M.A. Moore, G.A. Morris, Sample Convection in Liquid-State NMR: Why It Is Always with Us, and What We Can Do about It, J. Magn. Reson. 252 (2015) 120–129, https://doi.org/10.1016/j.jmr.2014.12.006.
[37] Morris, G. A.; Barjat, H. High Resolution Diffusion Ordered Spectroscopy. In Methods for Structure Elucidation by High-Resolution NMR; Batta, G., Kövér, K. E., Szántay Jr, C., Eds.; Elsevier, 1997; Vol. 8, pp 209–226. https://doi.org/10.1016/S0926-4345(97)80013-2.
[38] G.H. Sørland, J.G. Seland, J. Krane, H.W. Anthonsen, Improved Convection Compensating Pulsed Field Gradient Spin-Echo and Stimulated-Echo Methods, J. Magn. Reson. 142 (2) (2000) 323–325, https://doi.org/10.1006/jmre.1999.1941.
[39] A. Jerschow, N. Müller, Suppression of Convection Artifacts in Stimulated-Echo Diffusion Experiments, Double-Stimulated-Echo Experiments. J. Magn. Reson. 125 (2) (1997) 372–375, https://doi.org/10.1006/jmre.1997.1123.
[40] A. Jerschow, N. Müller, Convection Compensation in Gradient Enhanced Nuclear Magnetic Resonance Spectroscopy, J. Magn. Reson. 132 (1) (1998) 13–18, https://doi.org/10.1006/jmre.1998.1400.
[41] G. Stevanato, J.T. Hill-Cousins, P. Håkansson, S.S. Roy, L.J. Brown, R.C.D. Brown, G. Pileio, M.H. Levitt, A Nuclear Singlet Lifetime of More than One Hour in Room-Temperature Solution, Angew. Chemie Int. Ed. 54 (12) (2015) 3740–3743, https://doi.org/10.1002/anie.201411978.
[42] Long-Lived Nuclear Spin Order; Pileio, G., Ed.; New Developments in NMR; Royal Society of Chemistry: Cambridge, 2020. https://doi.org/10.1039/9781788019972.
[43] J. Eills, G. Stevanato, C. Bengs, S. Glöggler, S.J. Elliott, J. Alonso-Valdesueiro, G. Pileio, M.H. Levitt, Singlet Order Conversion and Parahydrogen-Induced Hyperpolarization of 13C Nuclei in near-Equivalent Spin Systems, J. Magn. Reson. 274 (2017) 163–172, https://doi.org/10.1016/j.jmr.2016.11.010.